Improved Palmprint Authentication using Contactless Imaging

Aythami Morales[1, 2], Miguel A. Ferrer[1], Ajay Kumar[2]
[1] Instituto Universitario para el Desarrollo Tecnológico y la Innovación en Comunicaciones (IDeTIC)
. Universidad de Las Palmas de Gran Canaria, Campus de Tafira, E35017 Las Palmas de Gran Canaria, Spain
[2]Department of Computing, The Hong Kong Polytechnic University, Hung Hom, Kowloon, Hong Kong
Email: amorales@gi.ulpgc.es, mferrer@dsc.ulpgc.es, ajaykr@ieee.org

***Abstract*—Palmprint identification has emerged as one of the popular and promising biometric modalities for forensic and commercial applications. In recent years the contactless system emerges as a viable option to address hygienic issues and improve the user acceptance. The presence of significant scale, rotation, occlusion and translation variations in the contactless palmprint images requires the feature extraction approaches which are tolerant to such changes. Therefore the usage of traditional palmprint feature extraction methods on contactless imaging schemes remains questionable and hence all/popular palmprint feature extraction methods may not be useful in contactless frameworks. This paper we systematically examine the issues related to the contactless palmprint authentication and presents performance evaluation on the two public databases. Our experimental results on more than 4300 images from two contactless databases suggests that the Scale Invariant Feature Transform (SIFT) features perform significantly better for the contactless palmprint images than the (most) promising Orthogonal Line Ordinal Features (OLOF) approach employed earlier on the more conventional palmprint imaging. Our experimental results further suggests that the combination of robust SIFT matching scores along with those from OLOF can be employed to achieve more reliable performance improvement. The achieved error rates show a good performance of these features in controlled and uncontrolled environments conditions with the error rates similar to other contact based approaches.**

I. INTRODUCTION

THE hand based biometric systems have invited increasing attention in last ten years. There are several approaches which presents promising results from hand geometry, fingerprint, palmprint, vein pattern or finger knuckles among other biometrics. The state of the art of hand based system goes from the earlier systems based on guiding pegs [1] to the pegfree systems robustness to hand and finger motion [2]. All these approaches present a contact surface to support the user hand during the acquisition. Therefore the contact between user and device is inevitable. The use of devices for applications with a large number of users raises hygienic concerns. The use of contactless system is the obvious solution to hygienic concerns. The absence of contact between the acquisition device and the user addresses the hygienic concerns and improve the user acceptability.

In the recent years, there have been several efforts to develop contactless biometric systems. In [3] was proposed a contactless biometric system based on a fusion of palm texture and palm vein pattern based on feature level and image level fusion. To realize the acquisition the user introduces the hand in a black box. Therefore illumination and background were controlled. The use of such black box can raise concerns or unwillingly scare the users and lower the user acceptance. In reference [4], the contactless hand geometry system able to obtain images in non controlled environments is investigated. The hand geometry based feature extraction methods show poor results due to projective distortion problems. Reference [15] examines the utility of SURF features for palmprint identification and presented promising results but on images acquired from flat bed scanner and portion of PolyU database using constrained imaging with user-pegs. The simultaneous use of 3D and 2D hand information was proposed in [5]. The images were acquired in contactless condition in a controlled scenario. The elevated cost of the 3D scanners is prohibitive for its possible current deployment but can it can be a possible solution in the near future.

The main difference between contact and contactless system lies in the significant intra-class variations generated by the absence of any contact or guiding contact surface. Such variations can result from the rotational and translation variations, projective distortion, scale variations, image blurring due to movement during the acquisition. The first question is therefore using better image normalization but the basic question is to ascertain how to extract the features which are invariant and robust to such variations from contactless imaging?

A. Our Work

In this paper we investigate the two feature extraction approaches for the contactless palmprint imaging. The first approach using SIFT is proposed to address the large intra-class variations from contactless imaging. We also examine the performance from possibly the best (as shown in [8]) approach in the palmprint literature using OLOF approach. The comparison between two such feature extraction methods could add more knowledge on the contactless palmprint systems behavior. Our experiments employ more than 4300 different images from two contactless databases acquired in controlled and uncontrolled environments conditions. These experimental results are significant and suggest that SIFT approach performs *significantly* better than OLOF approach that performed best among the several competitive approaches in [8]. The section B in this paper provides more detailed explanation on scale and rotational tolerance capabilities and experimental illustrations from real contactless images to ascertain such promises. However, the features extracted from SIFT and OLOF are complimentary and therefore it is judicious to

This work has been funded by Spanish government MCINN TEC2009-14123-C04 research project.

978-1-4244-7580-3/10/$26.00 ©2010 IEEE

combine these two observations and ascertain the further improvement in the performance.

II. Feature Extraction

The contactless images are characterized with the presence of severe rotation and scale changes, unlike those acquired from conventional systems based on the use of pegs or hand docking frame. The OLOF and SIFT feature investigation approach selected in this work are detailed in this section. The segmentation of region of interest from the contactless hand images, *i.e.* palmprint, is automatically achieved. The details for the method of segmentation are provided in the correspondent reference [7] which have developed respective database. In our work, we employ the contactless palmprint images of 150 × 150 pixels.

A. Modified SIFT (MSIFT)

The Scale Invariant Feature Transform was originally proposed in [12]. The features extracted are invariant to image scaling, rotation, and partially invariant to change in illumination and projective distortion. The SIFT is a feature extraction method based on the extraction of local information. The major stages to generate the set of features proposed by Lowe [9] are:

1) **Scale-space extrema detection:** It is applied over all scales and image locations. It is based on difference-of-Gaussian function to identify potential interest points that are invariant to scale and orientation. The input data is transformed to the space $L(x, y, \sigma)$ as follows:

$$L(x, y, \sigma) = G(x, y, \sigma) * I(x, y) \tag{1}$$

where $*$ corresponds to convolution operator, *I(x,y)* is the input image and $G(x, y, \sigma)$ is a Gaussian function with bandwidth σ.

$$D(x, y, \sigma) = \big(G(x, y, k\sigma) - G(x, y, \sigma)\big) * I(x, y) = \\ = L(x, y, k\sigma) - L(x, y, \sigma) \tag{2}$$

2) **Keypoint localization:** A detailed model is fit to determine location and scale of each candidate location. The interpolation is done using the quadratic Taylor expansion of the Difference-of-Gaussian scale-space function $D(x, y, \sigma)$ with the candidate keypoint as the origin. This Taylor expansion is given by:

$$D(x) = D + \frac{\partial D^T}{\partial x} + \frac{1}{2}\boldsymbol{x}^T \frac{\partial^2 D^T}{\partial x^2}\boldsymbol{x} \tag{3}$$

where D and its derivatives are evaluated at the candidate keypoint and $\boldsymbol{x} = (x, y, \sigma)$ is the offset from this point.

3) **Orientation assignment:** In our experiments we had used 16 orientations for each keypoint location based on local image gradient directions. For an image sample $L(x, y)$ at scale σ, the gradient magnitude, $m(x, y)$, and orientation, $\theta(x, y)$, are processed using pixel differences

$$m(x, y) = \sqrt{\big(L(x+1, y) - L(x-1, y)\big)^2 + \cdots \\ + \big(L(x, y+1) - L(x, y-1)\big)^2} \tag{4}$$

$$\theta(x, y) = tan^{-1}\left(\frac{L(x, y+1) - L(x, y-1)}{L(x+1, y) - L(x-1, y)}\right) \tag{5}$$

4) **Keypoint descriptor:** Around each keypoint, the local gradients are measured at the selected scale.

We propose to extract the keypoints from a Gabor filtered image instead of the grayscale image to add robustness to the feature extraction method. In Fig. 1 we show the different keypoints localization for a greyscale image and Gabor filtered image. It can be ascertained from these two images that the usage of even Gabor filters significantly improves the localization of palmprint lines, wrinkles and creases.

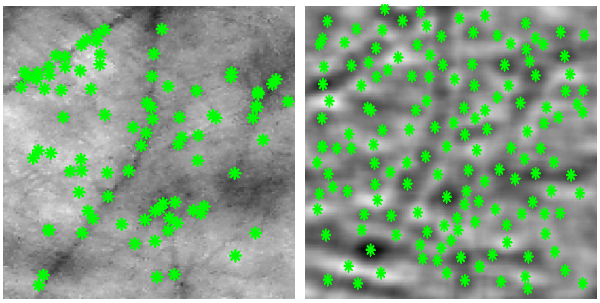

Figures 1: The extracted SIFT features over greyscale normalized touchless palm image, on the right SIFT features over corresponding Gabor filtered image.

The SIFT feature extraction method is the same in both cases and the difference is on the input image. On grayscale images the principals lines focus the keypoints localization. The principal lines may not be the most distinctive information on the contactless hand images and a more uniform distribution of the keypoints from principal lines, secondary lines, wrinkles, and creases can significantly improve the method performance. We obtain this uniform distribution filtering the grayscale image by using even Gabor filter. The use of this 2-D filter adds more robustness also against brightness variance on images. The filter parameters were same as in [11]. We did not apply any binarization after the filtering, we only normalize the filtered image.

Once the keypoints are extracted, the query image is matched and compared with each of the features extracted with the corresponding images in the registration database (from the training feature sets). The score generation from the candidate matches is based on Euclidean distance between the feature vectors.

B. OLOF

The Orthogonal Line Ordinal Features (OLOF) method was originally introduced in [8] and was investigated for the palmprint feature extraction. The comparison of OLOF method with several other competing methods [9]-[11] in this reference suggests the superiority of OLOF with such competitive feature extraction methods. The OLOF presented significantly improvement results but on conventional

databases that are acquired from constrained imaging. This method is based on 2D Gaussian filter to obtain the weighted average intensity of a line-like region. Its expression is as follows:

$$f(x,y,\theta) = \exp\left[-\left(\frac{x\cos\theta + y\sin\theta}{\delta_x}\right)^2 - \left(\frac{-x\sin\theta + y\cos\theta}{\delta_y}\right)^2\right] \quad (6)$$

where θ denotes the orientation of 2D Gaussian filter, δ_x denotes the filter's horizontal scale and δ_y denotes the filter's vertical scale parameter. We empirically selected the parameters as $\delta_x = 5$ and $\delta_y = 1$.

To obtain the orthogonal filter, two Gaussian filters are used as follows:

$$OF(\theta) = f(x,y,\theta) - f\left(x,y,\theta+\frac{\pi}{2}\right) \quad (7)$$

Each palm image is filtered using three ordinal filters, $OF(0)$, $OF(\pi/6)$, and $OF(\pi/3)$ to obtain three binary masks based on a zero binarization threshold. In order to ensure the robustness against brightness, the discrete filters $OF(\theta)$, are turned to have zero average.

Once filtered the palm image are resized to 50 × 50 pixels. The filtered images are used to compute the three ordinal feature matrix as shown in the following figure.

Figure 2: Ordinal feature matrix from a contactless palmprint image.

The matching distance between the palmprint image feature matrix Q and the palmprint image feature matrix P (say reference template) is computed by the normalized Hamming diatance which can be described as follows:

$$D = 1 - \frac{\sum_{i=1}^{2n+1}\sum_{j=1}^{2n+1} P(i,j) \otimes Q(i,j)}{(2n+1)^2} \quad (8)$$

where the boolean operator $\otimes$ is the conventional XOR operator. The numeric value of D ranges lies between 0-1 and the best matching is achieved when the value of D is 1. Because of the intra-class variations in the imaging and imperfections in preprocessing, the vertical and the horizontally translation ordinal feature map is used to ascertain the best possible matching scor. The ranges of the vertical, horizontal traslations and rotations are empirically determined and were fixed as from -6 to 6. The maximum D value obtained from such multiple translated matching is assigned as the best or final matching score.

III. Robustness of MSIFT Features and Fusion

In this section, we discuss and demonstrate the basic premise of our approach using SIFT and attempt to ascertain *why SIFT can be more useful for the contactless palmprint images as compared to other popular palmprint approaches*.

We use two normalized contactless palmprint images from two different subject and intentionally impart excessive scale and also rotational variation in one of the two images. We then comparatively evaluate the typical matching scores fromsuch images impaired by scale changes and rotational

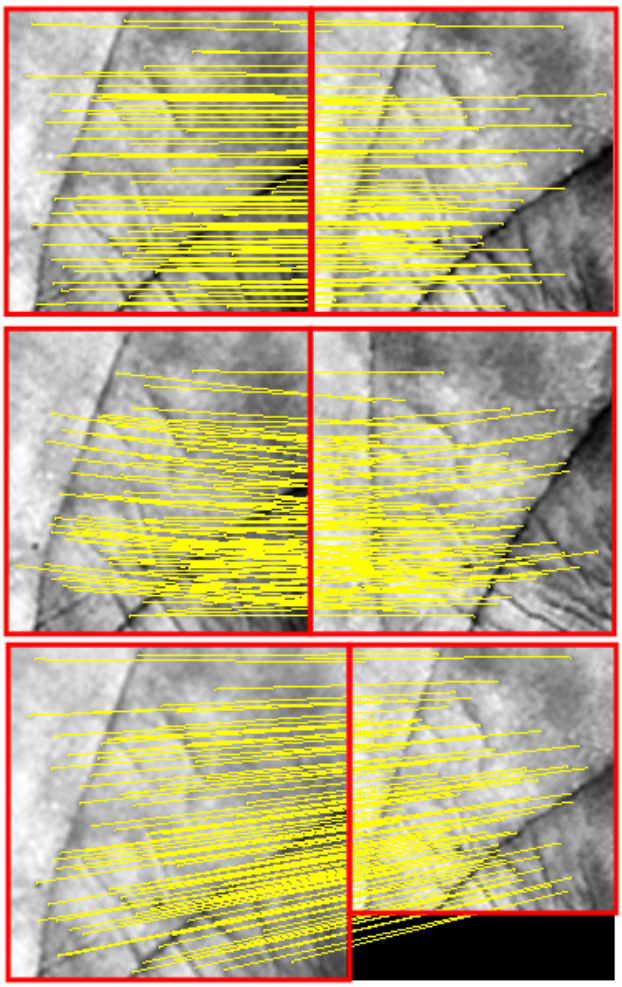

Figure 3: MSIFT robustness against rotation (20°) and scale variance (20% reduction). First row matches two images from same subject in contactless imaging; Second row matches the second image with a rotation of 20°; In third row the second image of same subject has 20% scale/size reduction.

changes (along with undistorted second image). The matching scores are computed using MSSIFT and OLOF approach. In the first experiment we used the original images and imparted 20% scale reduction representing inaccurate hand presentation scenario in contactless imaging. In addition, we introduced additional rotational distortion by 20° of rotation in the original image. The normalized scores obtained using MSIFT and OLOF are shown in Table 1. The robustness of MSIFT and OLOF with different distortions can also be observed from figure 3.

TABLE I: MATCHER ROBUSTNESS TO SCALE AND ROTATIONAL VARIATIONS

Distortion	MSIFT	OLOF
Original (no distortion)	**0.6190**	**0.6215**
Rotation (20°)	**0.3968** (35.9% ↓)	**0.0529**(91.48% ↓)
Scale (20%)	**0.5714** (7.69%↓)	**0.5118** (17.5% ↓)

A. *Matching Score Fusion*

The OLOF and SIFT scores were normalized based on *min-max* approach [16]. The consolidated matching scores were generated using the weighted sum approach as follows:

$$final\ score = wt' + (1 - w)s' \quad (9)$$

where *t'* is the normalized OLOF matching score and s' the normalized SIFT matching score. The weighted factor *w* is obtained during the training phase from the training samples (values between 0 and 1).

The figure 4-6 shows the distribution of genuine and imposter matching scores from the two feature extraction approaches. We can ascertain that the matching scores from the both features are widely separated. The distribution of matching scores also suggests that the matching scores from the two matchers are likely to be uncorrelated and therefore more effectively employed for combination [6].

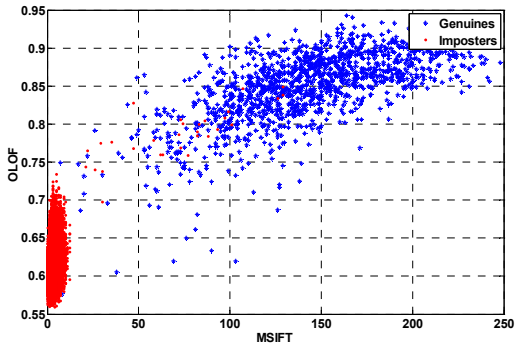

Figure 4: The distribution of matching scores for IITD database (Left).

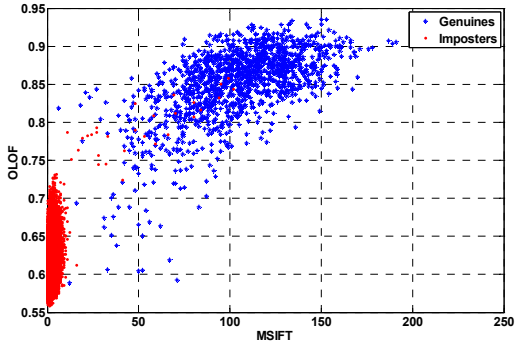

Figure 5: The distribution of matching scores for IITD database (Right).

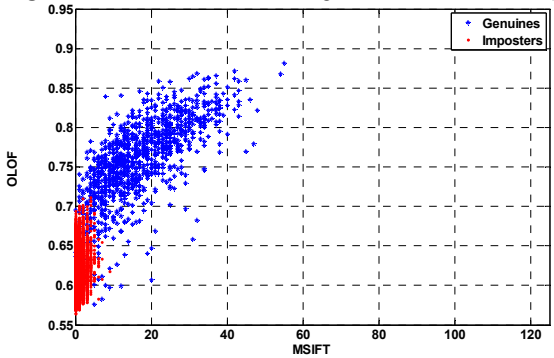

Figure 6: The distribution of matching scores for GPDS-CL database.

IV. DATABASES

In this work, we used two contactless databases acquired in controlled and uncontrolled conditions. By uncontrolled conditions we mean a database acquired in operative conditions with background and illumination unsupervised.

The IITD database is a publicly available database [17] and it consists of hand images with high projective, scale, rotational, and translational variations. The database is constituted from images from the left and right hands of 235 subjects. Considering each hand as an independent user, we have 470 different hands images with a minimum number of 6 images per user. The database was acquired in single sessions. As shown in figure 7, during the acquisition illumination and background conditions were quite controlled.

The GPDS-CL (Universidad de Las Palmas de Gran Canaria) database is a real application contactless database consists of 110 subjects imaging with average number of images per subject as 14. This database is divided in two kinds of user: habitual users and sporadic users. 70 habitual people used the system once per week during a four month period, this generated 10 sessions per user. The 40 sporadic people were acquired in 2 or 3 sessions. The training phase was supervised and the test phase was unsupervised. We had not rejected any of the images from the 4 month experiments. Some examples of acquired images can be seen in figure 7.

The main objective in building this database is to have large number of sessions and the unsupervised conditions for the imaging. This attempts to represent more realistic application environment. However the 110 subjects employed to build this database may not be enough to represent large population. In order to analyze the results from two contactless databases, the differences between both databases should be outlined. The main characteristics and differences between these two databases are summarized in the following table II.

TABLE II: MAIN CHARACTERISTICS OF GPDS-CL AND IITD DATABASES

Characteristics	GPDS-CL	IITD
Users	110	470(L+R)
Acquisitions per user	14	6
Sessions	3-10	1
Acquisition method	contactless	contactless
Background	uncontrolled	controlled
Illumination	uncontrolled	controlled
Image Resolution	800 × 600	800 × 600

In terms of projective, scale and blurred variation the GPDS-CL database show a greater variations and distortions in the acquired images.

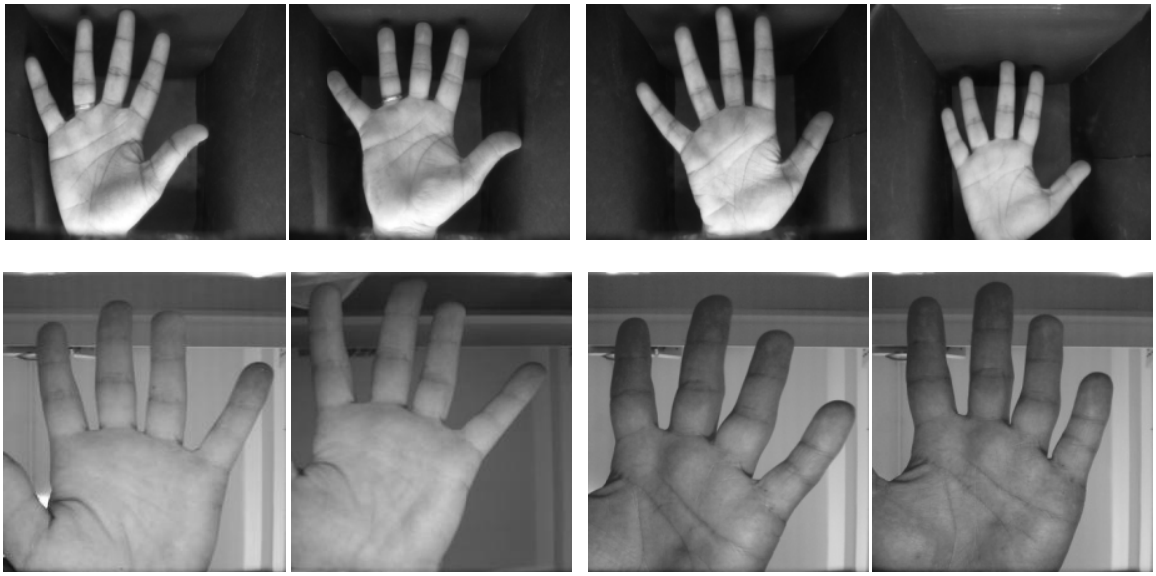

Figure 7: The images in first row are from two subjects in IITD touchless database while second row images are from two subjects in GPDS-CL database.

V. Experimental Results

The IITD images were acquired single sessions, therefore we used all the image in the performance evaluation. We used one image for test and the rest of the five images for the training. This was repeated five times, *i.e.*, cross-validation, and average of the experimental results are presented. For the GPDS-CL database we employed the first four images (from first session) as training samples and the rest of the images (rest of sessions) as test samples. We did not use images from different sessions for training to ascertain more realistic verification which can also account for the temporal variations introduced from time interval.

The common training methods used in some references employ imposters in the training phase. In several real applications, the system may not have information about the imposters. Therefore we attempt to ascertain more realistic results and divide the databases by users. We had used 20% of the users for training and 80% for test. We did not use information about the imposters in the training phase. The experimental results are reported by using the equal error rate (EER), the False Acceptance Rate (FAR) and False Rejection Rate (FRR) in the a priori user-independent thresholds, as shown in Table III-V.

TABLE III
AVERAGE PERFORMANCE (EER) FROM IITD RIGHT HAND

Matcher	EER(%)	User Independent a priori threshold FAR(%)	FRR(%)
MSIFT	0.39	0.50	0.31
OLOF	1.31	1.51	1.12
Fusion	0.21	0.36	0.16

The figure 8 and 9 shows the DET curves from of the IITD touchless palmprint database while figure 10 illustrates the

TABLE IV
AVERAGE PERFORMANCE (EER) FROM IITD LEFT HAND

Matcher	EER(%)	User Independent a priori threshold FAR(%)	FRR(%)
MSIFT	0.30	0.59	0.18
OLOF	0.61	0.65	0.59
Fusion	0.20	0.29	0.12

TABLE V
AVERAGE PERFORMANCE (EER) FROM GPDS-CL

Matcher	EER(%)	User Independent a priori threshold FAR(%)	FRR(%)
MSIFT	1.59	0.63	2.55
OLOF	2.25	2.44	2.06
Fusion	0.60	0.24	1.07

DET curves obtained from GPDS-CL database. The experimental results from our experiments summarized in Table III-V and figure 8-10 suggests that MSIFT approach significantly outperforms OLOF approach for authentication in contactless databases.

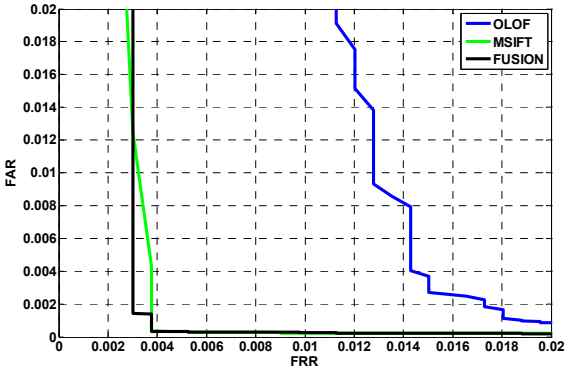

Figure 8: FAR and FRR for OLOF and MSIFT with IITD Right database.

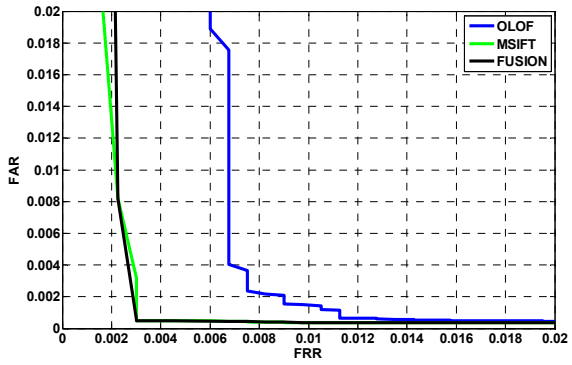

Figure 9: FAR and FRR for OLOF and MSIFT with IITD Left database.

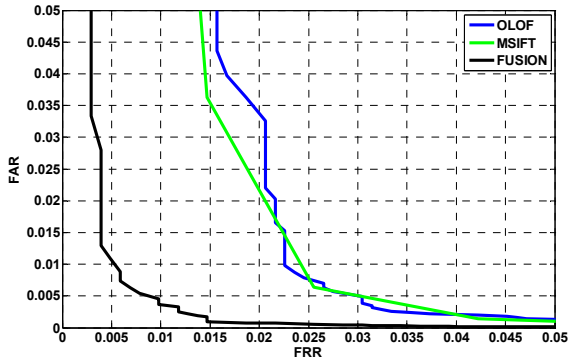

Figure 10: FAR and FRR for OLOF and MSIFT with GPDS-CL database.

VI. CONCLUSIONS

In this paper we systematically examined the contactless palmprint authentication and presented analysis of resulting image variations. The modified SIFT approach investigated in this paper outperforms the OLOF approach, primarily in presence of large intra-class variations resulting from the contactless imaging. Our experimental results on the two different contactless palmprint database suggests that the combination of modified SIFT and OLOF approach offers most promising alternative for more reliable contact less palmprint authentication.

TABLE V: RELATED WORK ON CONTACTLESS PALMPRINT AUTHENTICATION

Reference	Methodology	Database	Subjects	EER
[7]	Cohort Information	IITD [17]	235	1.31%
[14]	Palm and Knuckle	Proprietary	136	1.97%
[5]	2D and 3D Palm Features	Proprietary	177	2.6%
[18]	Homography using RANSAC	Proprietary	50	8.7%
[3]	Multispectral Palmprint	Proprietary	165	0.5%
This Paper	MSIFT and OLOF	IITD [17], GPDS-CL	235, 110	0.2%, 0.6%

This paper details experiments using two different contactless palmprint databases with more than 4300 images from 580 different hands. The images acquired in different condition achieve EER of 0.3% for controlled condition database and 0.6% for uncontrolled conditions database. In both cases the MSIFT method significantly improves the equal error rate as compared to those from OLOF method results. The reason of this improvement is due to the robustness of MSIFT against contactless variations. The contactless palmprint approaches have also been studied earlier. Reference [3] presented contactless palmprint authentication but employed multispectral images and its combination to achieve performance improvement. Table V presents a summary of related work on contactless palmprint authentication and illustrate lack of any effort to examine the strength of MSIFT features for contactless imaging. This paper has presented such experiments and presented promising results. Our further research efforts are focused to exploit the color information, which can also be simultaneously extracted during contactless palmprint imaging, and develop discriminant models to effectively assist in more reliable contactless palmprint identification.

REFERENCES

[1] A. Jain, A. Ross, and S. Pankanti, "A prototype hand geometry-based verification system," *Proc. 2nd Int. Conf. Audio- and Video-Based Biometric Person Authentication*, , pp. 166–171. Mar. 1999.

[2] G. Amayeh, G. Bebis, A. Erol, and M. Nicolescu, "Hand-Based Verification and Identification Using Palm-Finger Segmentation and Fusion," *Computer Vision and Image Understanding*, vol. 113, pp. 477-501, 2009.

[3] Y. Hao, Z. Sun, T. Tan and C. Ren, "Multi-spectral palm image fusion for accurate contact-free palmprint recognition," *Proc. ICIP 2008*, pp. 281-284, 2008.

[4] A. Morales, M. A. Ferrer j.B. Alonso, C. M. Travieso, "Comparing infrared and visible illumination for contactless hand based biometric scheme," *Proc. 42nd Annual IEEE International Carnahan Conference*, on Security Technology, ICCST 2008. pp. 191 – 197, 2008.

[5] V. Kanhangad, A. Kumar, D. Zhang, "Combining 2D and 3D hand geometry features for biometric verification," *Proc. CVPRW 2009*. pp. 39 – 44, 2009.

[6] K. Nandakumar, Y. Chen, S. C. Dass and A. K. Jain, "Likelihood ratio based biometric score fusion," *IEEE Trans. Pattern Anal. Mach. Intell.*, vol. 30, pp. 342-347, Feb. 2008.

[7] A. Kumar, "Incorporating Cohort Information for Reliable Palmprint Authentication," *Proc. ICVGIP 2008*, pp 112-119, Bhubaneswar (India), Dec. 2008.

[8] Z. Sun, T. Tan, Y. Wang, and S. Z. Li, "Ordinal palmprint representation for personal identification,", *Proc. CVPR 2005*, vol. 1, pp. 279- 284, 2005.

[9] D. Zhang, W. Kong, J. You, and M. Wong, "OnlinePalmprint Identification," *IEEE Trans. PAMI*, vol. 25,no. 9, pp. 1041-1050, 2003.

[10] P. Hennings and V. Kumar, "Palmprint classification using pattern-specific segmentation and optimal correlation filters," *IEEE Trans. Info. Forensics & Security*, vol. 2, no. 3, Sept. 2007.

[11] W.K. Kong and D. Zhang, "Competitive Coding Scheme for Palmprint Verification," *Proc. of the 17th ICPR*, vol.1, pp. 520-523, 2004.

[12] D. G. Lowe, "Distinctive image features from scale-invariant keypoints," *IJCV*, vol. 2, no. 60, pp. 91 110, 2004.

[13] J. Chen and Y. S. Moon, "Using SIFT features in palmprint authentication," *Proc. 19th ICPR 2008*, pp. 1-4, Dec. 2008.

[14] G. K. Ong Michael, T. Connie, A. T. B. Jin, "An innovative contactless palmprint and knuckle print recognition system," *Pattern Recognition Lett.*, to appear, 2010.

[15] G. S. Badrinath, P. Gupta, "Robust Biometric System Using Palmprint for Personal Verification" *Proc. ICB 2009*, Vol. 558, pp. 554-565, 2009.

[16] A. K. Jain, K. Nandakumar, and A. Ross, "Score normalization in multimodal biometric systems," *Pattern Recognition*, vol. 38, 2005.

[17] IITD Touchless Palmprint Database, Version 1.0 (available online): http://web.iitd.ac.in/~ajaykr/Database_Palm.htm.

[18] C. Methani, A. M. Namboodiri, "Pose invariant palmprint recognition", *Proc. ICB 2009*, pp. 577-586, Jun. 2009.